Study the nonlinear behavior of MWCNTs and ZnO/Se/MWCNTs

Conference Paper *in* AIP Conference Proceedings · July 2019

DOI: 10.1063/1.5117016

3 authors:

Zainab Sabeeh Sadeq
University of Baghdad, College of Science
44 PUBLICATIONS **187** CITATIONS
SEE PROFILE

Saif Alshrefi
University of Babylon
19 PUBLICATIONS **148** CITATIONS
SEE PROFILE

Dunia Kamil
University of Baghdad
43 PUBLICATIONS **103** CITATIONS
SEE PROFILE

Study the nonlinear behavior of MWCNTs and ZnO/Se/MWCNTs

Cite as: AIP Conference Proceedings **2123**, 020089 (2019); https://doi.org/10.1063/1.5117016

Zainab S. Sadeq, Saif M. Alshrefi, and Dunia K. Mahdi

AIP Conference Proceedings **2123**, 020089 (2019); https://doi.org/10.1063/1.5117016 **2123**, 020089

Study the Nonlinear Behavior of MWCNTs and ZnO/Se/MWCNTs

Zainab S. Sadeq[1, a)], Saif M. Alshrefi [2], Dunia K. Mahdi [1]

[1]*University of Baghdad - College of Science- Department of Physics, Baghdad, Iraq.*
[2] *University of Babylon - College of Science for Women - Department of Laser Physics, Hilla City, Babylon, Iraq.*

a) zainab.sabeeh@scbaghdad.edu.iq

Abstract. MWCNTs and hybrid nanocomposite ZnO/Se/MWCNTs have been prepared via Solvothermal technique using Parr reactor at the temperature 180°C and $SeCl_2$ as a catalyst. The obtained MWCNTs and ZnO/Se/MWCNTs are investigated using the FE-SEM, XRD, UV-VIS Spectroscopy and Z-Scan. The novelty of this research is studying the nonlinear optical properties for these prepared materials and the results exhibit that the thickness of the deposited film for hybrid nanocomposite ZnO/Se/MWCNTs is increased, which in turn, increase the nonlinear phase shift of the laser beam compared with the MWCNTs.

Keywords: Hybrid Materials doped with MWCNTs, nonlinear optical properties.

INTRODUCTION

Carbon nanotubes were discovered by S. Iijima [1], who was looking for new CSs, in the deposit formed on graphite cathode surfaces during the discharge which is, employed to prepare of fullerene soot. The CNTs, also known as tubular fullerenes, are cylindrical graphene sheets of sp^2 bonded the carbon atoms. Nanotubes are concentric graphitic cylinders with the closed end due to the presence of five-membered rings. The CNTs, can be multi-walled with a central tube of nanometric diameter surrounded by graphitic layers [2]. Since the discovery of CNTs, various methods of preparing them have been reconnoitered and synthesized carbon nanotubes by various techniques like arc-discharge, Laser Evaporation, Chemical Vapor Deposition (CVD), High-Pressure carbon monoxide method (HiPco), The unique catalyst mixture of Cobalt and Molybdenum used (CoMoCat), Laser Ablation and Solvothermal technique [3,4], etc. These techniques are very beneficial and are of extended importance. The CNTs can have a high aspect ratio, low mass density, high tensile strength, the large surface area, high heat conductivity and versatile electronic behavior, including high electron conductivity [5,6]. The advantage of liquid hydrocarbons as carbon source is that they're the cheap and controlled insertion of the liquid additive are often introduced into the reactor wherever they kind active carbon species for carbon CN's growth were the type of catalysts that affects the morphology and crop of carbon nanotubes [7]. This work involves using a low-cost method to prepare MWCNTs and hybrid nanocomposite ZnO/Se/MWCNTs to study the nonlinear optical properties.

MATERIALS AND METHODS

The chemicals in this research supported from (VWR Company) with purity (99.9%).

Preparation of MWCNTs

Typically, 70 ml of Ethyl alcohol, 30 ml of water, 7gm of KOH, 3gm PEG of 14.000Mw and 1 gm PMMA Polymer, were added to Becker of 200 ml and mixed using magnetic stirrer for 30 min. After that, 0.2 gm of Selenium

Technologies and Materials for Renewable Energy, Environment and Sustainability
AIP Conf. Proc. 2123, 020089-1–020089-6; https://doi.org/10.1063/1.5117016
Published by AIP Publishing. 978-0-7354-1863-9/$30.00

Dichloride, which is used as a catalyst, dissolved in 10 ml DW, still under magnetic stirrer for 1 hr. Then mixed the above two solutions and transferred to 250 ml Homemade Parr reactor Teflon Jar (Homemade locally in Georgia Institute of Technology-MSE, Georgia, USA). After that, the reactor was sealed and maintained at 180 ºC for 24 hr in a furnace, then, the reactor cooled down to room temperature, and the product wash four times with water and alcohol. Lastly, the prepared sample was dried using vacuum oven at 65 ºC for 8hr.

Preparation of hybrid Nanocomposite ZnO/Se/MWCNTs

Also, Solvothermal method have been used to hybrid Zinc Oxide (ZnO) and Selenium NPs with MWCNTs using two solutions. The first solution was resolve 4 gm of KOH in 10 ml of DW, also 4gm of ZnO nm (grain size: 30-40 nm) resolve in 20ml of DW. Then the second solution was resolve 0.2 gm of $SeCl_2$ in 10 ml of DW. Finally, mixed all the above solutions and transfer them to the Autoclave under 180°C for 24 hr with immerse piece of high carbon steel inside Teflon Jar of the Autoclave to increase the encouraging combined ZnO with MWCNTs. Then all the prepared samples were cool down to room temperature. The prepared nanocomposite was washed with water and alcohol for several times and dried at 65 °C for 24 hr.

RESULTS AND DISCUSSION

The FE-SEM images of the MWCNTs and ZnO/Se/MWCNTs were taken by (Zeiss ULTRA 60 FE-SEM, at the Georgia Tech./MSE.-USA). The prepared MWCNTs length diameters was up to several micrometers as in figure 1-a. The time is enough to prepare a chain of MWCNTs, also when temperature increase leads to particle size increase (i.e., small surface area). The interface connection between Se NPs and ZnO NPs can clearly be observed as in figure 1-b, ZnO NPs to closely the surface of $SeCl_2$ because of the piece of steel inside Teflon jar attracts ingredients floating in solution and shows the role of Iron (Fe: appear in the XRD pattern in figure 2-a), Nickel (Ni: appear in the XRD pattern in figure 2-a) and Cobalt (Co) elements within its structure knitting to connect the components in the reaction environment. The image of ZnO/Se/MWCNTs shows the porous structures in the ZnO NPs, which can contribute to a large surface area which agree with other research's results [7-12]. Some ZnO and Se NPs were closely linked to the surface of ZnO/Se/MWCNTs, as in figure 1-c. MWCNTs had close contact with ZnO NPs in the hybrid nanocomposite, the diameter of the coated MWCNTs increases and the inner core of MWCNTs is hardly visible which have a particle diameter within the range of (36–51) nm with average lengths of (1.5–2) µm, and (20-42) nm for Se with the mean particle size (36.30-56.53) nm for ZnO/Se/ MWCNTs and mean particle size (45-55) nm for ZnO, which measured by FE-SEM device directly.

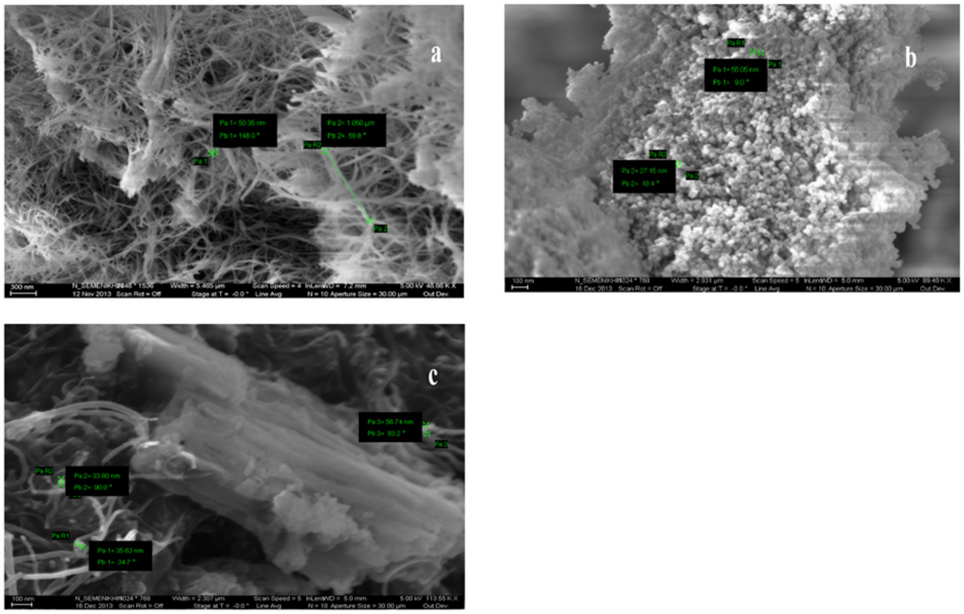

FIGURE 1: FE-SEM images of : a) MWCNTs, b) ZnO-$SeCl_2$, c) ZnO/Se/MWCNTs.

The (XRD) pattern of the samples were analysis using X-ray diffractometer equipped with Cu-Ka radiation (λ=1.5406 Å) as in figure 2. Diffraction peaks indexed (1 0 0), (1 0 1), (1 1 0), (1 0 2), (2 0 0) and (2 0 0) can be assigned as cubic close-packed (Se) and also the other diffraction peak at 26.5° are indexed to (0 0 2) are point out to graphene layers. The above results ensure the reduction reaction of potassium hydroxide to potassium and disintegrate chemical compound C2H5O- K+ to C2H5O- and K+, once it mixed with the PEG & PMMA presence of pressure and heat caused polymerization.

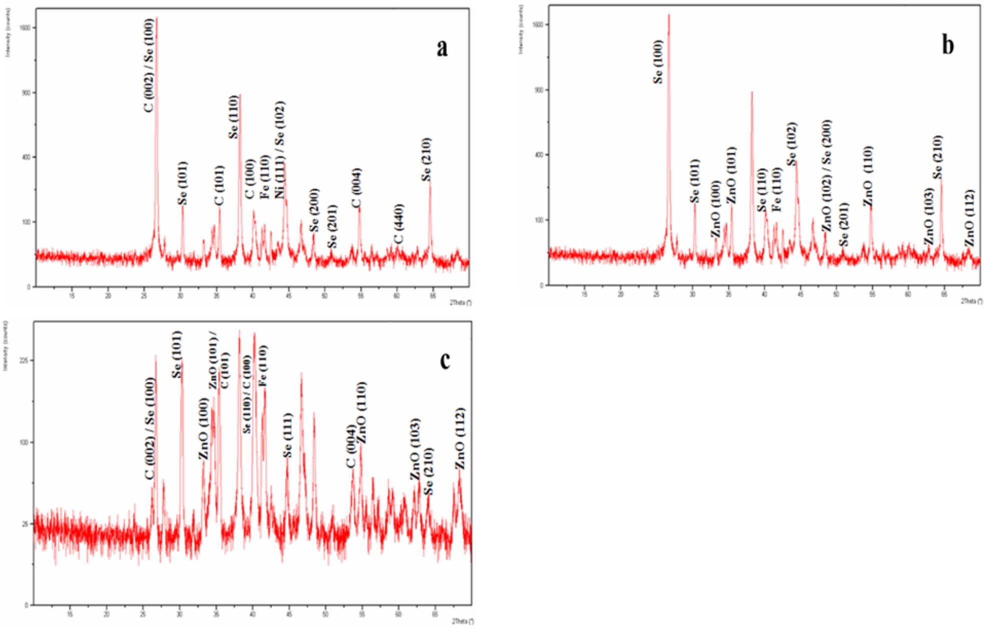

FIGURE 2: The XRD pattern of: a) MWCNTs, b) ZnO/Se, c) ZnO/Se/MWCNTs Nanocomposites.

XRD pattern shows two strong peaks for (0 0 2) which indicates that (1 0 0) is the radial direction of MWCNTs and it indicates grown from the catalytic particles [8-11]. ZnO/Se/MWCNTs nanocomposites were of the homogeneous structure with crystallinity, and the average crystallite sizes which calculated from the Scherrer equation were found to be about 30.86-56 nm. The two peaks overlapped at $2\theta = 25.9°$ can be found easily and clearly in the Se NPs-coated by MWCNTs and two weak peaks at $2\theta = 41.3°$ which convergent with Rodrigues O. E. D.et al, [12]. This main peak overlapped with that of ZnO and MWCNTs at $2\theta = 34.8°$.

An enhancement of absorption can be seen for ZnO/Se/MWCNTs composite material compared with pure MWCNTs as shown in figure 3. A significant blue shift within the visible region less than 500 nm in a little bit is observed for ZnO/Se/MWCNTs. Also, the absorption spectrum shows scattering in the range of 370–392 nm due to formation nano-clusters of MWCNTs in the ZnO matrix compared with other results [12-15].

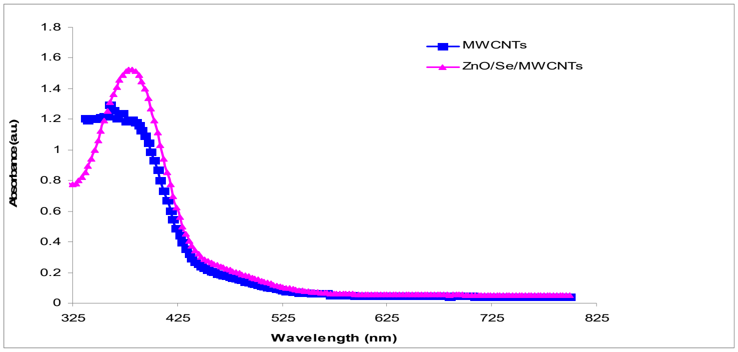

FIGURE 3: UV-Visible spectra of MWCNTs and ZnO/Se/MWCNTs composite.

The nonlinear optical (NLO) properties which include the nonlinear refractive index (n_2) and nonlinear absorption coefficient (β) were investigated for Multi-Walled Carbon Nano-Tubes (MWCNTs) and ZnO/Se/MWCNTs composite (Hybrids) by the Z-Scan technique with Nd: YAG pulsed Laser at the wavelength of 532 nm and intensity 6.794 GW/cm^2. Two methods were used to measure the NLO properties of materials, the closed-aperture and the open-aperture of Z-Scan. The first one, which used to calculate the n_2, where an aperture, is placed behind prepared samples within the far field to manage the cross sectional σ of the beam which coming out of the sample. As the prepared samples are scanned through the beam, the profile of far field displays the variation of intensity across the beam profile, that is recorded via the aperture and also the transmission, is recorded as a function of (Z-position). Figure 4 exhibit the results for the closed aperture of Z-scan for MWCNTs and ZnO/Se/MWCNTs composite (Hybrids). Where this figure shows a refractive index of negatives singes (peak to valley) for optical nonlinear z-scan which represents the effect of self-defocusing for MWCNTs and ZnO/Se/MWCNTs composite, and this profile of Z-scan starting far from the focus (**$z < 0$**), the flounce of the beam is low and nonlinear refraction is negligible, i.e., z-independent. As the MWCNTs and ZnO/Se/MWCNTs composite approaches the beam focus, intensity will increase, resulting in self-lensing in the above samples tend to collimate the beam on the aperture within the far field, leading to increase the transmittance which calculated at the iris position as Luděk Bartoněk & Jiří Keprt mentioned [16].

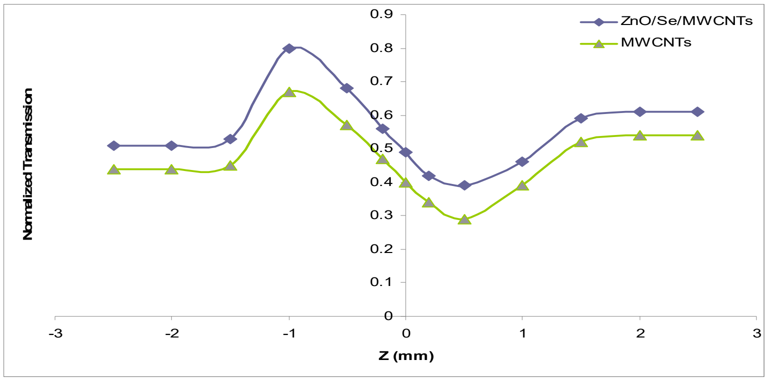

FIGURE 4: The closed aperture of Z-Scan for MWCNTs and ZnO/Se/MWCNTs composite (Hybrids).

After the focal plane, the effect of the self-defocusing leading to increases the divergence beam, and this causes, a widening of the beam at the iris which in turn lead to reducing the measured transmittance. Again, at $z > 0$, the n_2 is low resulting , i.e., z-independent. It is clear from the figure 4, the Z-scan results varies for both MWCNTs and ZnO/Se/MWCNTs composite because the difference of concentration of additives in each film caused variation in films thickness, increasing caused the increase of the laser beam phase shift, which lead to change the nonlinear phase shift ($\Delta\Phi_o$) which intern changes the value of n_2 and the third order electric susceptibility [17]. It is observed that, with the condition of small $\Delta\Phi_o$, the curves profile of Z-scan is approximately symmetric, where the increase and decrease of normalized intensity at the aperture are basically the same as Alessandra Micoli mentioned [18]. As seen from the table 1, that the relation between the $\Delta\Phi_o$ and the **n_2** is linearly increasing relation and determined from equation (1) [19].

$$\mathbf{n_2 = \Delta\Phi_o \,/\, I_o L_{eff}\, k} \qquad \text{.... (1)}$$

Where $\mathbf{k = 2\pi / \lambda}$

λ is the wavelength of the beam.

I_o is the intensity at the focal spot given by

L_{eff}: The effective length of the prepared materials which can be determined from equation (2).

$$\mathbf{L_{eff} = (1 - e^{-\alpha o L}) / \alpha_o} \qquad \text{.... (2)}$$

where,

L is the sample length,

α_o is linear absorption coefficient

TABLE 1: Nonlinear refractive index for MWCNTs and ZnO/Se/MWCNTs composite (Hybrids) using the closed aperture of Z-scan.

Samples	α_o	$\Delta\Phi_o$	n_2 type	n_2 cm^2/ GW
MWCNTs	**230430**	**0.9359**	**–ve**	**0.273**
ZnO/Se/MWCNTs	**219101.3**	**1.0098**	**–ve**	**0.279**

The open aperture of Z-scan was used to calculate the nonlinear absorption coefficient (β) by removing the aperture, which leading to collecting all the transmitted light [19,20]. The figure 5 shows the open aperture of Z-scan results for MWCNTs and ZnO/Se/MWCNTs nanocomposite (Hybrids).

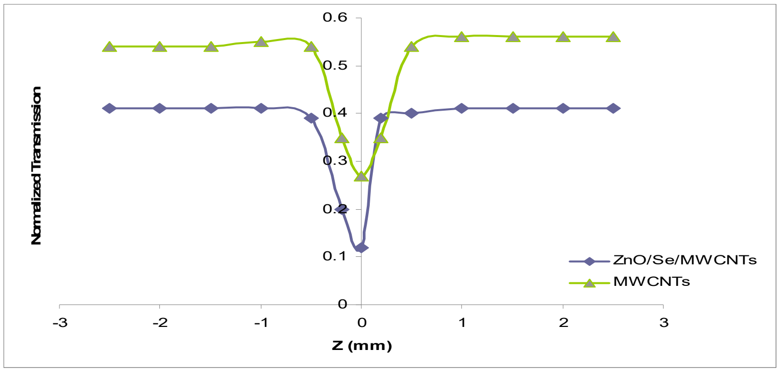

FIGURE 5: The open aperture of Z-Scan for MWCNTs and ZnO/Se/MWCNTs nanocomposite.

Figure 5 shows negative asymmetric valley observed at minimum transmittance (T_{min}), where Z = 0 mm, which indicates a two-photon absorptions (TPA) in the prepared materials when travels through the beam waist. The open-aperture of Z-scan defines variable transmittance values, which used to calculate the β [19,20]. The table 2 listed the variable transmittance values of MWCNTs and ZnO/Se/MWCNTs composite (Hybrids) to determine β (which determined from equation (3)) at the wavelength of 532 nm with the intensity of 6.794 GW/cm².

$$T(Z) = \sum_{m=0}^{\infty} \frac{\left[\frac{\beta I_0 L_{eff}}{1+(Z/Z_0)^2}\right]^m}{(m+1)^{3/2}} \qquad \ldots (3)$$

where

Z is the sample position at the minimum transmittance

Z_o is the diffraction length

m is integer

T(z) is the minimum transmittance

TABLE 2: Nonlinear absorption coefficient for MWCNTs and ZnO/Se/MWCNTs composite (Hybrids) using the open aperture of Z-scan.

Samples	L_{eff} (cm)	T_{min}	β (cm/GW)
MWCNTs	**4.27 x 10^{-6}**	**0.27**	**67164.54675**
ZnO/Se/MWCNTs	**4.51 x 10^{-6}**	**0.12**	**36887.47273**

CONCLUSION

The novelty of this work is using the solvothermal technique to prepare MWCNTs and hybrid nanocomposite of ZnO/Se/MWCNTs by low-temperature to explain the nonlinear optical properties for MWCNTs and ZnO/Se/MWCNTs. The nonlinear refractive index exhibits the effect the self - defocusing for the closed aperture of Z-scan, whiles, the open aperture of Z-scan exhibits reversed saturable absorption (indicating the two-photon absorption).

REFERENCES

1. P. Poncharal, Z.L. Wang, D. Ugarte, and W. A. D. Heer, Electrostatic deflections, and electromechanical resonances of carbon nanotubes, Science 283, 1513–1516 (1999).
2. S. Iijima, Helical microtubules of graphitic carbon, Nature 354, 56–64 (1991).
3. C.D. Scott, S. Arepalli, P. Nikolaev and R. E. Smalley, Growth mechanism for single-wall carbon nanotubes in a laser ablation process, Applied Physics A 72, 573-580 (2001).
4. D. S. Bethune, C. H. Kiang, M. S. de Vries, G. Gorman, R. Savoy, J. Vazquez and R. Beyers, Cobalt-catalysed growth of carbon nanotubes with single-atomic-layer walls, Nature 363, 605-607 (1993).
5. B.W. Smith, M. Monthioux, D.E. Luzzi, Encapsulated C60 in carbon nanotubes, Nature 396, 323-324 (1998).
6. J.M. Calderon-Moreno, M. Yoshimura, Hydrothermal processing of high-quality multiwall nanotubes from amorphous carbon, Journal of American. Chemistry Society 123, 741–743 (2001).
7. Saif M. Alshrefi, Dunia K. Mahdi, Zainab S. Sadik, Synthesis of TiO2/Pd/Multi-Walled Carbon Nano-Structures by Hydrothermal Technique and deposited it on n-Si substrate as TiO2/Pd/MWCNTs:n-Si Heterojunction by Pulsed Laser Deposition, Eng. &Tech. Journal 33 Part (B) 867-883 (2015).
8. D. Gültekin, M. Altaf and H. Akbulut, Synthesis and Characterization of ZnO Nanopowders and ZnO-CNT Nanocomposites Prepared by Chemical Precipitation Route, ACTA PHYSICA POLONICA A, A123, 274-276 (2013).
9. N. Wang, Z. K. Tang, G. D. Li, and J. S. Chen, Single-walled 4Å carbon nanotube arrays, Journal of Nature 408, 50-51 (2000).
10. Wenzhong Wang, J.Y. Huang, D.Z. Wang and Z.F. Ren, Low-temperature hydrothermal synthesis of multiwall carbon nanotubes, Letters to the Editor, Carbon 43, 1328-1331 (2005).
11. F. Alkaim , Zainab Sadik, D. K Mahdi, S. M Alshrefi, A. k. M. Al-Sammarraie, F. M. Alamgir, P. M. Singh, and A. M. Aljeboree, “Preparation, structure and adsorption properties of synthesized multiwall carbon nanotubes for highly effective removal of maxilon blue dye”, Korean J. Chem. Eng., 32, 2456-2462 (2015).
12. M. Ahmad, E. Ahmed, Z.L. Hong, W. Ahmed, A. Elhissi and N.R. Khalid, Photocatalytic, sonocatalytic and sonophotocatalytic degradation of Rhodamine B using ZnO/CNTs composites photocatalysts, Journal of Ultrasonics Sonochemistry 21, 761-773 (2014).
13. O. E. D. Rodrigues, G. D. Saraiva, R. O. Nascimento, E. B. Barros, J. Mendes Filho, Y. A. Kim, H. Muramatsu, M. Endo, M. Terrones, M. S. Dresselhaus and A. G. Souza Filho, Synthesis and Characterization of Selenium-Carbon Nanocables, Journal of Nano Letters 8, 3651-3655 (2008).
14. Yun Ye, Shoujin Cai, Min Yan, Tianyuan Chen, Tailiang Guo, Concentration detection of carbon nanotubes in electrophoretic suspension with UV–Vis. spectrophotometry for application in field emission devices. College of Physics and Information Engineering, Fuzhou University, China, ELSEVIER Pub., J. of Applied Surface Science 284, 107-112 (2013).
15. Sourabh Dwivedi, Abdul Aziz A. Al Khedhairy, Maqusood Ahamed and Javed Musarrat, Biomimetic Synthesis of Selenium Nanospheres by Bacterial Strain JS-11 and Its Role as a Biosensor for Nanotoxicity Assessment: A Novel Se-Bioassay, Journal of PLoS One 8, 1-10 (2013).
16. Luděk Bartoněk and Jiří Keprt, Application of computer-processed video signal in the optics of thin films. Proce. SPIE 4356, 12th Czech-Slovak-Polish Optical Conference on Wave and Quantum Aspects of Contemporary, (2001).
17. M. Mansoor Sheik-Bahae, A. A. Said, D. J. Hagan, M. J. Soileau, and S. E. Van Stryland, Nonlinear refraction and optical limiting in thick media, Optical engineering 30, 1228-1235 (1991).
18. Alessandra Micoli PhD Thesis (Università degli Studi di Trieste, Italy) (2012).
19. Zainab S. Sadeq, Dhia H. Al-Amiedy and Amal F. Jaffar, Third Order Optical Nonlinearities of C450 Doped Polymer Thin Film Investigated by the Z-Scan, Advances in Materials Physics and Chemistry 2, 43-49 (2012).
20. Zainab Sabeeh Sadeq, Non Linear Optical Properties of Silver Nanoparticles, Iraqi Journal of Science 57 3C, 2240-2244 (2016).